

Fig. S1. FTIR spectrum of LDH

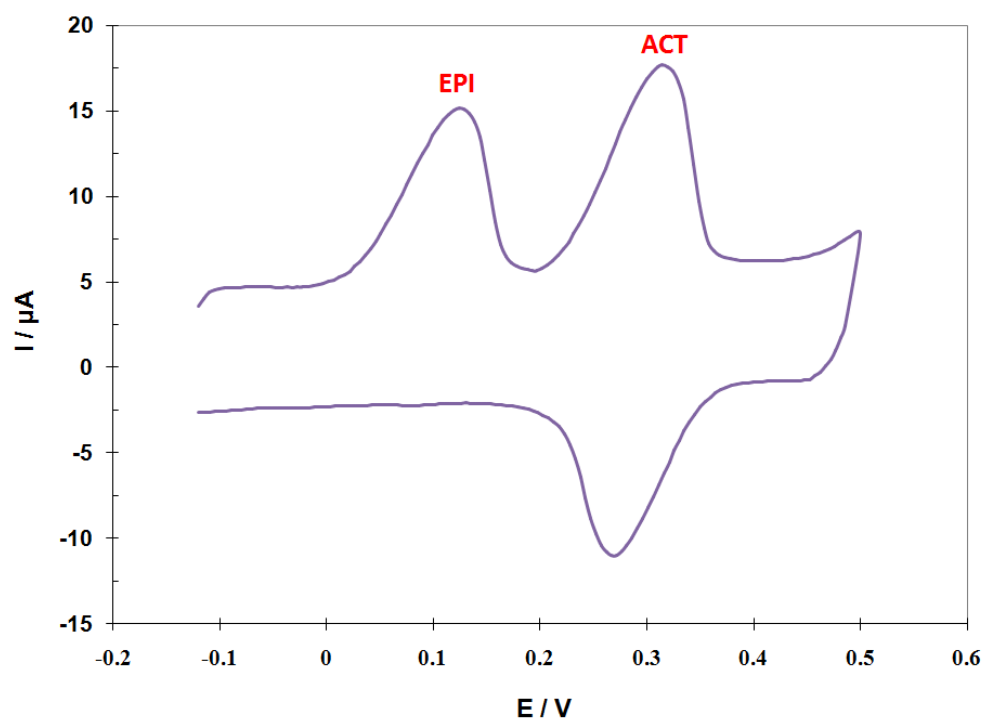


Fig. S2. Cyclic voltammogram of simultaneous determination of 5 μM EPI and 5 μM ACT at MWCNTs-NHNPs-LDH/GCE in 0.1 mol L⁻¹ phosphate buffer solution (pH=7) at scan rate of 50 mVs⁻¹.

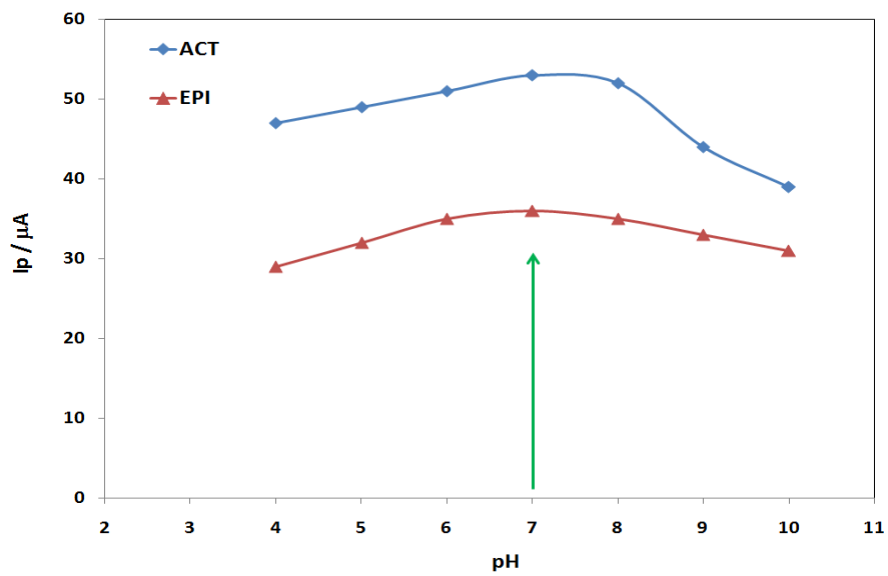


Fig. S3. Plot of anodic peak currents (I_{pa}) as a function of pH of buffer solutions for 20 μM EPI and 20 μM ACT compounds at MWCNTs-NHNPs-LDH/GCE in 0.1M phosphate buffer.

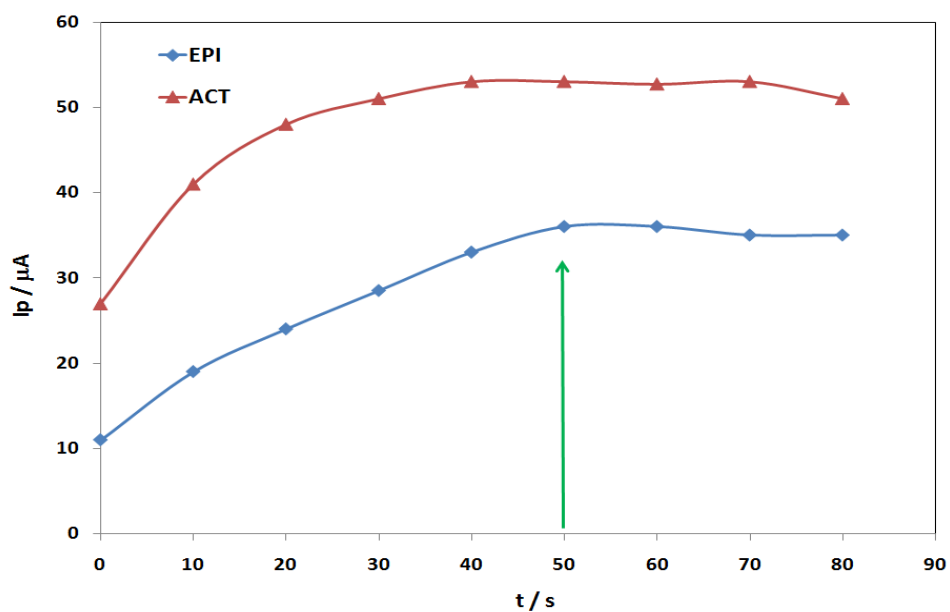


Fig. S4. Plot of anodic peak currents (I_p) as a function of accumulation time for 20 μM EPI and 20 μM ACT compounds at MWCNTs-NHNPs-LDH/GCE in 0.1M phosphate buffer.

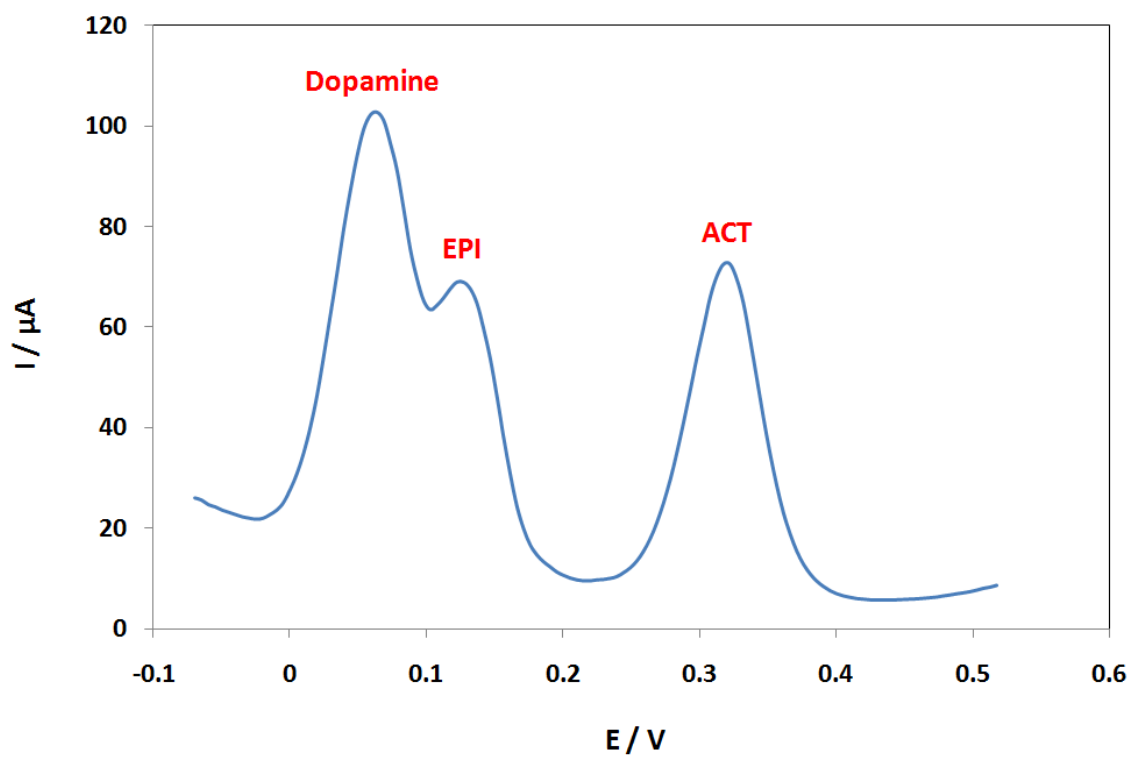


Fig. S5. Differential pulse voltammogram of 40 μM EPI and 30 μM ACT at MWCNTs-NHNPs-LDH/GCE in present of 200 μM Dopamine.

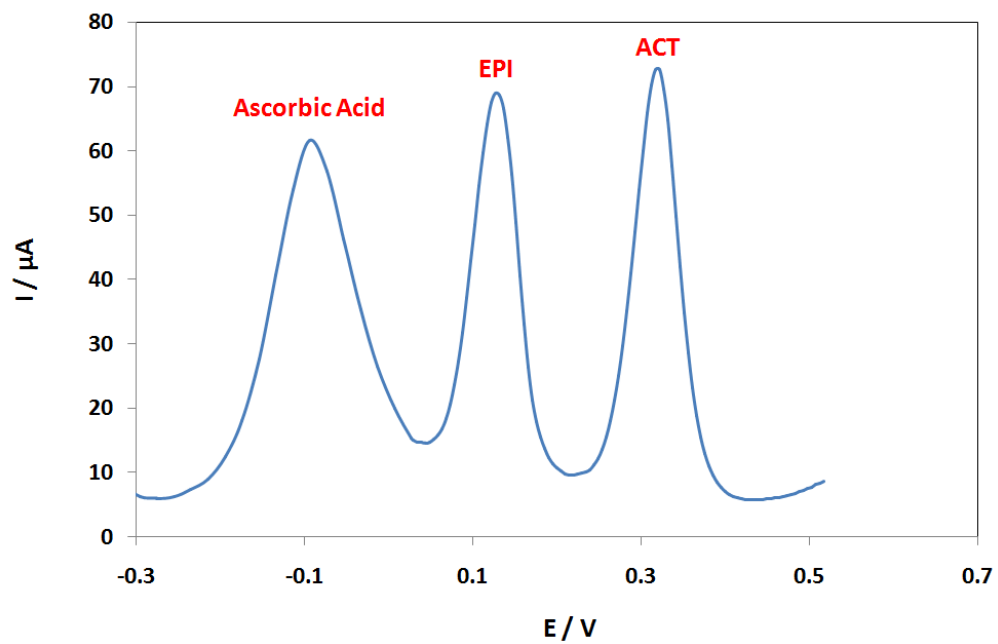


Fig. S6. Differential pulse voltammogram of 40 μM EPI and 30 μM ACT at MWCNTs-NHNPs-LDH/GCE in present of 350 μM ascorbic acid.

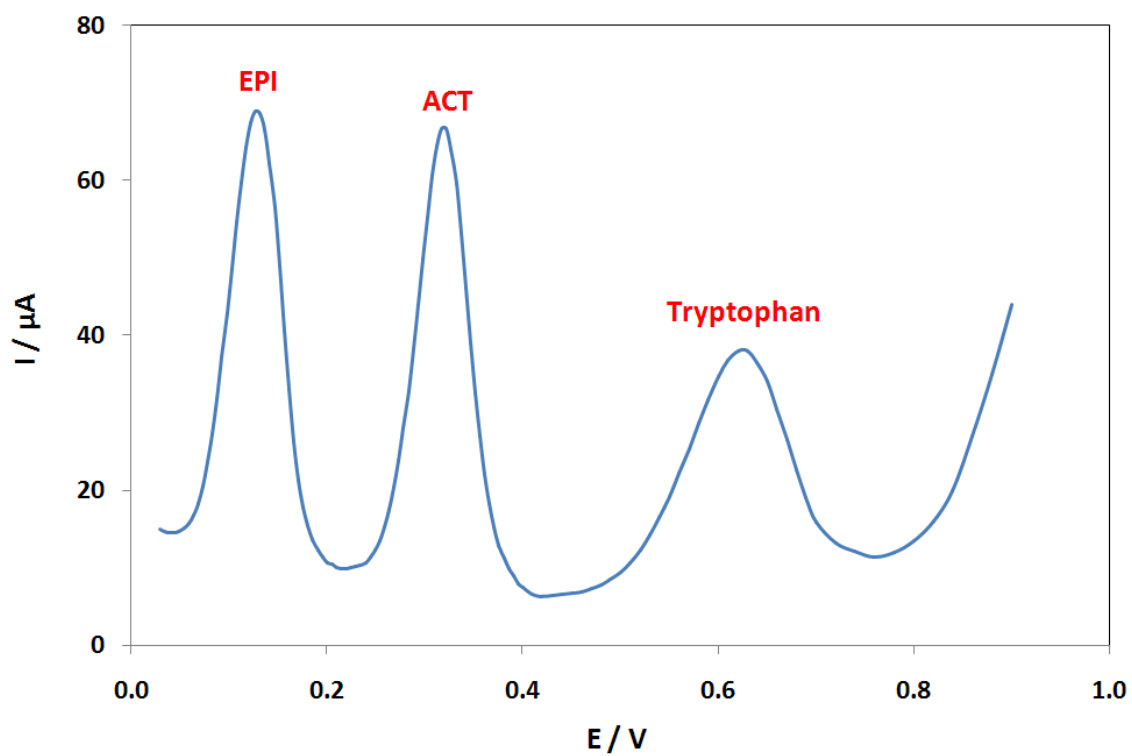


Fig. S7. Differential pulse voltammogram of 40 μM EPI and 30 μM ACT at MWCNTs-NHNPs-LDH/GCE in present of 250 μM Tryptophan.

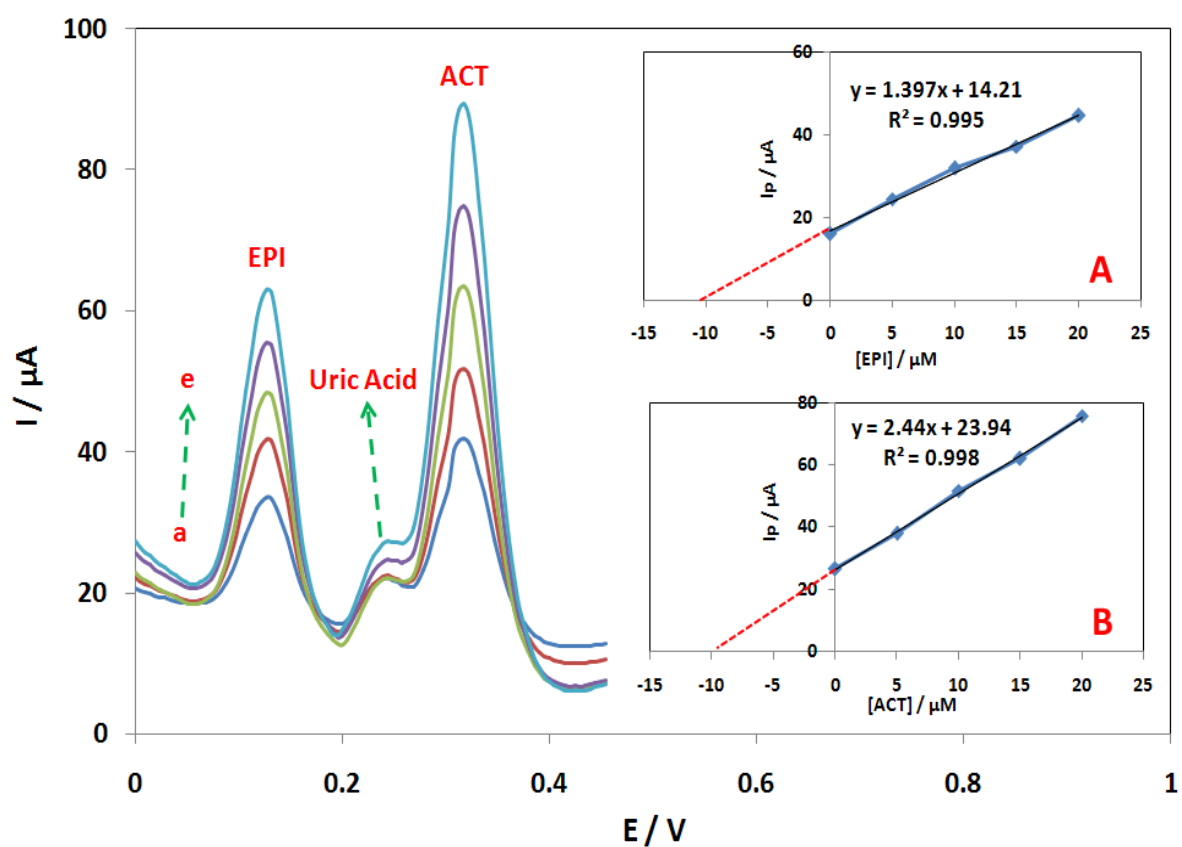


Fig. S8. Differential pulse voltammograms of variously spiked concentrations of EPI and ACT mixtures in human blood serum containing 10 μM EPI and 10 μM ACT at the surface of MWCNTs-NHNPs-LDH/GCE: (a) 0+0, (b) 5+5, (c) 10+10, (d) 15+15 and (e) 20+20 μM . Insets: (A) calibration curve of EPI and (B) calibration curve of ACT.

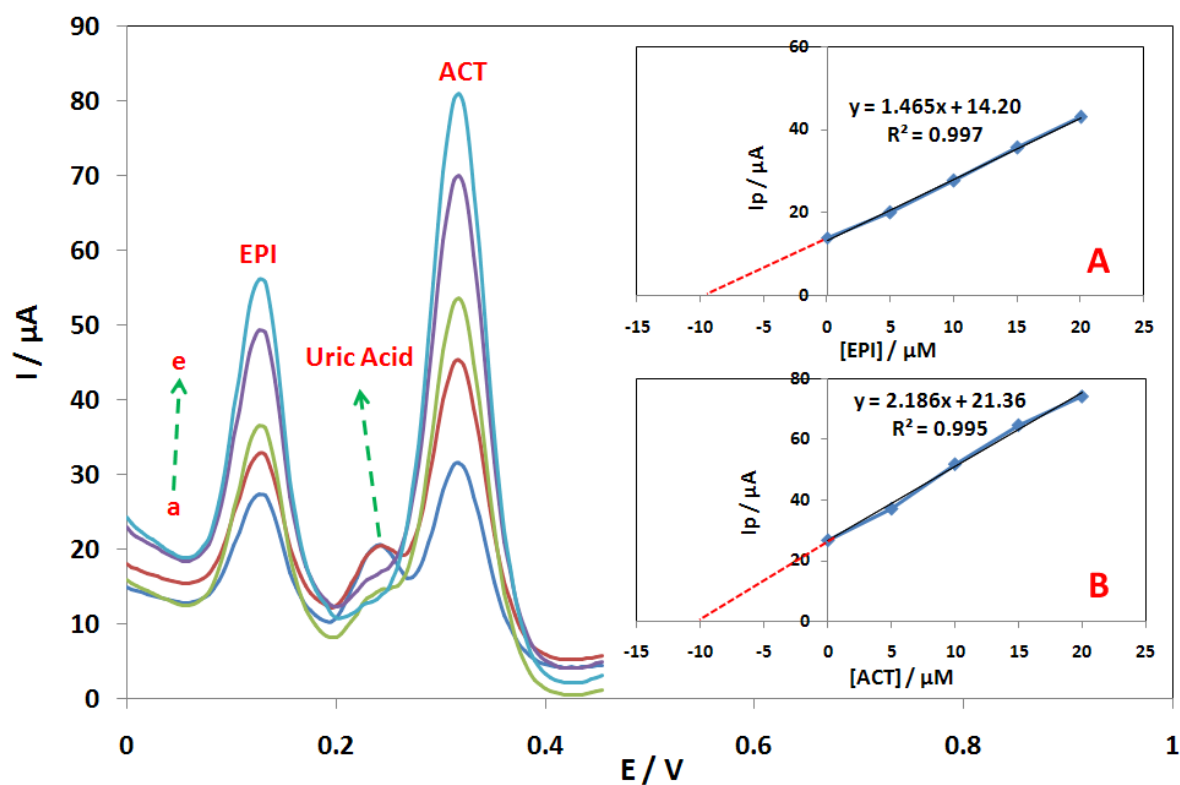


Fig. S9. Differential pulse voltammograms of variously spiked concentrations of EPI and ACT mixtures in human urine containing 10 μM EPI and 10 μM ACT at the surface of MWCNTs-NHNPs-LDH/GCE: (a) 0+0, (b) 5+5, (c) 10+10, (d) 15+15 and (e) 20+20 μM . Insets: (A) calibration curve of EPI and (B) calibration curve of ACT.